Higgs Boson Pair Production in Gluon Fusion at Next-to-Leading Order with Full Top-Quark Mass Dependence

S. Borowka, N. Greiner, G. Heinrich, S. P. Jones, M. Kerner, J. Schlenk, U. Schubert, and T. Zirke

Phys. Rev. Lett. **117**, 012001 — Published 29 June 2016

DOI: 10.1103/PhysRevLett.117.012001

MPP-2016-80, NSF-KITP-16-040, ZH-TH-14/16

Higgs boson pair production in gluon fusion at NLO with full top-quark mass dependence

S. Borowka
Institute for Physics, Universität Zürich, Winterthurerstr.190, 8057 Zürich, Switzerland and Kavli Institute for Theoretical Physics, University of California, Santa Barbara, CA 93106, USA

N. Greiner
Institute for Physics, Universität Zürich, Winterthurerstr.190, 8057 Zürich, Switzerland

G. Heinrich, S. P. Jones, M. Kerner, J. Schlenk, U. Schubert, and T. Zirke
Max Planck Institute for Physics, Föhringer Ring 6, 80805 München, Germany
(Dated: June 10, 2016)

We present the calculation of the cross section and invariant mass distribution for Higgs boson pair production in gluon fusion at next-to-leading order (NLO) in QCD. Top-quark masses are fully taken into account throughout the calculation. The virtual two-loop amplitude has been generated using an extension of the program GoSam supplemented with an interface to Reduze for the integral reduction. The occurring integrals have been calculated numerically using the program SecDec. Our results, including the full top-quark mass dependence for the first time, allow us to assess the validity of various approximations proposed in the literature, which we also recalculate. We find substantial deviations between the NLO result and the different approximations, which emphasizes the importance of including the full top-quark mass dependence at NLO.

INTRODUCTION

The couplings of the Higgs boson to electroweak bosons and heavy fermions are being established as Standard-Model-like at an impressive rate. In contrast, the measurement of the Higgs boson self-coupling, which is vital in order to confirm the mechanism of electroweak symmetry breaking, is still outstanding, and will have to wait until the LHC high-luminosity upgrade. However, the Higgs boson self-coupling(s) could be enhanced by physics Beyond the Standard Model (BSM), and it is an important task to be able to distinguish BSM effects from effects due to higher order corrections in perturbation theory.

Gluon fusion is the dominant production channel for Higgs boson pair production. However, as this process proceeds via a heavy quark loop already at the leading order (LO), the next-to-leading order corrections involve two-loop four-point diagrams with two masses, m_h and m_t, and the analytic calculation of two-loop four-point integrals with different internal and external mass scales has not been achieved so far.

The leading order (one-loop) calculation of Higgs boson pair production in gluon fusion has been performed in Refs. [1, 2]. NLO corrections in the $m_t \to \infty$ limit for both the Standard Model and the MSSM have been performed in Ref. [3]. Finite top-quark mass corrections to the NLO result have been calculated in Refs. [4–9]. The NNLO QCD corrections in the $m_t \to \infty$ effective field theory also have been computed [6, 10, 11], and they have been supplemented by an expansion in $1/m_t^2$ in Ref. [8]. In the effective field theory, resummation at NLO+NNLL has been considered in Ref. [12], and recently, even matched NNLO+NNLL resummed results became available [13]. The dominant uncertainty therefore is given by the unknown top-quark mass effects at NLO.

The top-quark mass effects have been included in various approximations in the literature:

(i) The "Born-improved HEFT (Higgs Effective Field Theory)" approximation, which is the one employed in the program Hpair [2, 3]. It uses the heavy top-quark limit throughout the NLO calculation, in combination with a re-weighting factor B/B_{HEFT}, where B denotes the leading order result in the full theory. In Hpair the re-weighting is done at matrix element level, but after the angular integration of the phase space, while in Ref. [7] it is done on an event-by-event basis.

(ii) The "FT_{approx}" result of Refs. [5, 7] contains the full top-quark mass dependence in the real radiation, while the virtual part is rescaled by the re-weighting factor mentioned above.
It was found that (ii) leads to a total cross section which is about 10% smaller than the one obtained using Born-improved HEFT.

(iii) The "FT'_{approx}" result [7] is as in (ii) for the real radiation part, while it uses partial NLO results for the virtual part, specifically, the exact results for the two-loop triangle diagrams as far as they are known from single Higgs boson production [14–17].

(iv) HEFT results at NLO and NNLO have been improved by an expansion in $1/m_t^{2\rho}$ in Refs. [4, 6, 8, 9],

where Ref. [8] contains corrections up to $\rho^{\max} = 6$ at NLO, and $\rho^{\max} = 2$ for the soft-virtual part at NNLO. In Ref. [8] it is also demonstrated that the sign of the finite top-quark mass corrections depends on whether the re-weighting factor is applied at differential level, i.e. before the integration over the partonic center of mass energy, or at total cross section level.

All these results suggest that the uncertainty on the cross section due to top-quark mass effects is $\pm 10\%$ at NLO.

In this letter we present results for the total cross section and the Higgs boson pair invariant mass distribution for the process $gg \to hh$ at NLO, including the full top-quark mass dependence. The analytically unknown two-loop integrals have been calculated numerically with the program SecDec [18–20]. Our results settle the long-standing question about the uncertainty related to the various approximations which have been calculated so far.

NLO CALCULATION

Amplitude structure

At any loop order, the amplitude for the process $g(p_1) + g(p_2) \to h(p_3) + h(p_4)$ can be decomposed into form factors as

$$\mathcal{M}_{ab} = \delta_{ab}\epsilon_1^\mu \epsilon_2^\nu \mathcal{M}_{\mu\nu} \tag{1}$$
$$\mathcal{M}^{\mu\nu} = F_1(\hat{s},\hat{t},m_h^2,m_t^2,D)\, T_1^{\mu\nu} + F_2(\hat{s},\hat{t},m_h^2,m_t^2,D)\, T_2^{\mu\nu} ,$$

where $\epsilon_1^\mu, \epsilon_2^\nu$ are the gluon polarization vectors, a, b are colour indices, and

$$\hat{s} = (p_1+p_2)^2, \quad \hat{t} = (p_1-p_3)^2, \quad \hat{u} = (p_2-p_3)^2 . \tag{2}$$

The decomposition into tensors carrying the Lorentz structure is not unique. With the following definitions

$$T_1^{\mu\nu} = g^{\mu\nu} - \frac{p_1^\nu p_2^\mu}{p_1\cdot p_2} , \tag{3}$$
$$T_2^{\mu\nu} = g^{\mu\nu} + \frac{1}{p_T^2\,(p_1\cdot p_2)}\,\tilde{T}_2^{\mu\nu} ,$$
$$\tilde{T}_2^{\mu\nu} = \big\{ m_h^2\, p_1^\nu p_2^\mu - 2\,(p_1\cdot p_3)\, p_3^\nu p_2^\mu - 2\,(p_2\cdot p_3)\, p_3^\mu p_1^\nu + 2\,(p_1\cdot p_2)\, p_3^\nu p_3^\mu \big\} ,$$
$$\text{where} \quad p_T^2 = (\hat{t}\hat{u} - m_h^4)/\hat{s} ,$$
$$T_1\cdot T_2 = D-4 ,\ T_1\cdot T_1 = T_2\cdot T_2 = D-2 ,$$

we have [1]

$$\mathcal{M}^{++} = \mathcal{M}^{--} = -F_1 ,\ \mathcal{M}^{+-} = \mathcal{M}^{-+} = -F_2 . \tag{4}$$

At leading order, we can further split F_1 into a triangle diagram and a box diagram contribution, $F_1 = F_\triangle + F_\square$. As the form factor $F_\triangle$ only contains the triangle diagrams, which have no angular momentum dependence, it can be attributed entirely to an s-wave contribution. The form factor F_2 contains only box contributions. At NLO in QCD, the feature persists that only F_1 contains diagrams involving the triple Higgs coupling. The form factors F_1 and F_2 can be attributed to the spin-0 and spin-2 states of the scattering amplitude, respectively.

We construct projectors $P_j^{\mu\nu}$ such that

$$P_1^{\mu\nu}\mathcal{M}_{\mu\nu} = F_1(\hat{s},\hat{t},m_h^2,m_t^2,D) ,$$
$$P_2^{\mu\nu}\mathcal{M}_{\mu\nu} = F_2(\hat{s},\hat{t},m_h^2,m_t^2,D) .$$

For the projectors in D dimensions we can use as a basis the tensors $T_i^{\mu\nu}$ defined in Eqs. (3). The projectors can be written as

$$P_1^{\mu\nu} = \frac{1}{4}\frac{D-2}{D-3}\,T_1^{\mu\nu} - \frac{1}{4}\frac{D-4}{D-3}\,T_2^{\mu\nu} , \tag{5}$$
$$P_2^{\mu\nu} = -\frac{1}{4}\frac{D-4}{D-3}\,T_1^{\mu\nu} + \frac{1}{4}\frac{D-2}{D-3}\,T_2^{\mu\nu} . \tag{6}$$

LO cross section

The partonic leading order cross section can be written as

$$\hat{\sigma}^{\rm LO} = \frac{1}{2^9\,\pi\,\hat{s}^2}\int_{\hat{t}_-}^{\hat{t}_+} d\hat{t}\,\Big\{|F_1|^2 + |F_2|^2\Big\}, \tag{7}$$

where

$$\hat{t}^\pm = m_h^2 - \frac{\hat{s}}{2}\,(1 \mp \beta_h) ,\ \beta_h^2 = 1 - 4\frac{m_h^2}{\hat{s}} . \tag{8}$$

The leading order form factors F_i with full mass dependence can be found e.g. in Refs. [1, 2].

For the total cross section, we also have to integrate over the parton distribution functions, so we have

$$\sigma^{\rm LO} = \int_{\tau_0}^1 d\tau\ \frac{d\mathcal{L}_{gg}}{d\tau}\ \hat{\sigma}^{\rm LO}(\hat{s}=\tau s) . \tag{9}$$

The luminosity function is defined as

$$\frac{d\mathcal{L}_{ij}}{d\tau} = \sum_{ij}\int_\tau^1 \frac{dx}{x} f_i(x,\mu_F) f_j\left(\frac{\tau}{x},\mu_F\right), \tag{10}$$

where s is the square of the hadronic centre of mass energy, $\tau_0 = 4m_h^2/s$, μ_F is the factorization scale and f_i are the parton distribution functions (PDFs) for parton type i.

NLO cross section

The NLO cross section is composed of various parts, which we will discuss separately in the following:

$$\sigma^{\rm NLO}(pp\to hh) = \sigma^{\rm LO} + \sigma^{\rm virt} + \sum_{i,j\in\{g,q,\bar{q}\}}\sigma_{ij}^{\rm real} \tag{11}$$

The virtual two-loop amplitude

For the virtual two-loop amplitude, we use the projectors defined in Eqs. (5),(6) to express the amplitude in terms of the scalar form factors F_1 and F_2.

The virtual amplitude has been generated with an extension of the program GoSam [21, 22], where the diagrams are generated using Qgraf [23] and then further processed using Form [24, 25]. This leads to about 10000 integrals before any symmetries are taken into account. The two-loop extension of GoSam contains an interface to Reduze [26], which we used for the reduction to master integrals. We have defined 8 integral families with 9 propagators each. For the 6 and 7 propagator non-planar topologies we could not achieve a complete reduction with our available computing resources using the reduction programs Reduze [26], Fire [27] or LiteRed [28]. In this case we evaluated the tensor integrals directly, exploiting the fact that SecDec can calculate integrals with (contracted) loop momenta in the numerator.

After the partial reduction, we end up with 145 planar master integrals plus 70 non-planar integrals and a further 112 integrals that differ by a crossing. As the master integrals contain up to four independent mass scales, $\hat{s}$, $\hat{t}$, m_t^2, m_h^2, only a small subset is known analytically. Therefore we have calculated all the integrals numerically using the program SecDec-3.0 [20]. We partially used a finite basis [29] for the planar master integrals, as far as it turned out to be beneficial for the numerical integration.

The interface to SecDec has been constructed such that the coefficients of the master integrals as they occur in the amplitude are taken into account when evaluating the integrals numerically. For each integral, once a relative accuracy of 0.2 is reached, the number of sampling points is then set dynamically according to two criteria: (i) the contribution of the integral including its coefficient to the error estimate of the amplitude and (ii) the time per sampling point spent on the integral. The numerical integration is continued until the desired precision for the full amplitude is reached. This procedure allows for a precise evaluation of the amplitude, without spending an unnecessary amount of time on individual integrals which are suppressed in the full amplitude.

For the numerical integration we use a quasi-Monte Carlo method based on a rank-one lattice rule [30–32]. For suitable integrands, this rule provides a convergence rate of $\mathcal{O}(1/n)$ as opposed to Monte Carlo or adaptive Monte Carlo techniques, such as Vegas [33], which converge $\mathcal{O}(1/\sqrt{n})$, where n is the number of sampling points. The integration rule is implemented in OpenCL 1.1 and a further (OpenMP threaded) C++ implementation is used as a partial cross-check. The 665 phase-space points used for the current publication were computed with ∼16 dual Nvidia Tesla K20X GPGPU nodes using a total of 4680 GPGPU hours.

We use conventional dimensional regularization (CDR) with $D = 4 - 2\epsilon$. The top-quark mass is renormalized in the on-shell scheme and the QCD coupling in the $\overline{\text{MS}}$ scheme with $N_f = 5$. The top-quark mass counterterm is obtained by insertion of the mass counterterm into the heavy quark propagators. Alternatively, the mass counterterm can be calculated by taking the derivative of the one-loop amplitude with respect to m_t. We have used both methods as a cross-check.

Real radiation

The contributions from the real radiation, $\sigma_{ij}^{\text{real}}$, can be divided into four channels, according to the partonic subprocesses $gg \to hh+g, gq \to hh+q, g\bar{q} \to hh+\bar{q}, q\bar{q} \to hh+g$. The $q\bar{q}$ channel is infrared finite.

We have generated the one-loop amplitudes for all subprocesses with the program GoSam [21, 22]. For the subtraction of the infrared poles, we use the Catani-Seymour dipole formalism [34]. Further we use a phase-space restriction parameter α to limit the subtractions to a smaller region in phase space, as suggested in Ref. [35]. We have retained the full top-quark mass dependence throughout the calculation of the $2 \to 3$ matrix elements and IR subtraction terms. For the phase-space integration we use the Vegas algorithm [33] as implemented in the Cuba library [36].

The infrared poles of the virtual contribution $\mathrm{d}\hat{\sigma}^{\text{virt}}$ cancel in the combination $(\mathrm{d}\hat{\sigma}^{\text{virt}} + \mathrm{d}\hat{\sigma}^{\text{LO}} \otimes \mathbf{I})$, where the $\mathbf{I}$-operator is given by

$$\mathbf{I} = \frac{\alpha_s}{2\pi} \frac{(4\pi)^\epsilon}{\Gamma(1-\epsilon)} \left(\frac{\mu^2}{\hat{s}}\right)^\epsilon \left\{ \frac{2C_A}{\epsilon^2} + \frac{\beta_0}{\epsilon} + \text{finite} \right\} . \quad (12)$$

Checks

We have checked that for all calculated phase space points the numerical cancellations of the poles in ϵ are within the numerical uncertainties. For a randomly chosen sample of phase-space points we calculated the poles with higher accuracy and obtained a median cancellation of five digits.

Our implementation of the virtual two-loop amplitude is checked to be invariant under the interchange of $\hat{t}$ and $\hat{u}$ by recomputing 10 randomly selected phase-space points. The part of the amplitude known from single Higgs boson production is checked against the program of Ref. [17]. Further, the one-loop amplitude is computed using an identical framework to the two-loop amplitude and is checked against the result of Ref. [1].

We have verified the independence of the amplitude from the phase space restriction parameter α. Further, we have compared to the results of Ref. [7] for the approximations (i) and (ii) mentioned above, and found agreement within the numerical uncertainties [37].

As a further cross-check we have also calculated mass corrections as an expansion in $1/m_t^2$ in the following way: we write the partonic differential cross section as

$$d\hat{\sigma}_{\text{exp},N} = \sum_{\rho=0}^{N} d\hat{\sigma}^{(\rho)} \left(\frac{\Lambda}{m_t}\right)^{2\rho} , \tag{13}$$

where $\Lambda \in \left\{\sqrt{\hat{s}}, \sqrt{\hat{t}}, \sqrt{\hat{u}}, m_h\right\}$, and determine the first few terms (up to $N = 3$) of this asymptotic series with the help of QGRAF [23], Q2E/EXP [38, 39] and MATAD [40], as well as REDUZE [26] and FORM [24, 25].

We applied the series expansion to the virtual corrections, combined with the infrared insertion operator $\mathbf{I}$, such that the expression in brackets below is infrared finite,

$$\begin{aligned} &d\hat{\sigma}^{\text{virt}} + d\hat{\sigma}^{\text{LO}}(\epsilon) \otimes \mathbf{I} \\ &\approx \left(d\hat{\sigma}^{\text{virt}}_{\text{exp},N} + d\hat{\sigma}^{\text{LO}}_{\text{exp},N}(\epsilon) \otimes \mathbf{I}\right) \frac{d\hat{\sigma}^{\text{LO}}(\epsilon)}{d\hat{\sigma}^{\text{LO}}_{\text{exp},N}(\epsilon)} , \end{aligned} \tag{14}$$

such that we can set $\epsilon = 0$ in $d\hat{\sigma}^{\text{LO}}/d\hat{\sigma}^{\text{LO}}_{\text{exp},N}$. There is some freedom when to do the rescaling, i.e. before/after the phase-space integration and convolution with the PDFs. We opt to do it on a fully differential level, i.e. the rescaling is done for each phase-space point individually. The comparison of this expansion with the full result is shown in the next section.

NUMERICAL RESULTS

In our numerical computation we set $\mu_R = \mu_F = \mu = m_{hh}/2$, where m_{hh} is the invariant mass of the Higgs boson pair. We use the PDF4LHC15_nlo_100_pdfas [41–44] parton distribution functions, along with the corresponding value for α_s for both the LO and the NLO results. The masses have been set to $m_h = 125\,\text{GeV}$, $m_t = 173\,\text{GeV}$, and the top-quark width has been set to zero. We use a centre-of-mass energy of $\sqrt{s} = 13\,\text{TeV}$ and no cuts except a technical cut in the real radiation of $p_T^{\text{min}} = 10^{-4} \cdot \sqrt{\hat{s}}$, which we varied in the range $10^{-2} \leq p_T^{\text{min}}/\sqrt{\hat{s}} \leq 10^{-6}$ to verify that the contribution to the total cross section is stable and independent of the cut within the numerical accuracy.

Including the top-mass dependence, we obtain the total cross section at $\sqrt{s} = 13\,\text{TeV}$

$$\sigma^{NLO} = 27.72^{+13.7\%}_{-12.7\%}\,\text{fb} \pm 0.4\%\,(\text{stat.}) \pm 0.1\%\,(\text{int.}).$$

In addition to the dependence of the result on the variation of the scales by a factor of two around the central scale, we state the statistical error coming from the limited number of phase-space points evaluated and the error stemming from the numerical integration of the amplitude. The latter value has been obtained using error propagation and assuming Gaussian distributed errors and no correlation between the amplitude-level results. The value of the cross section is 14% smaller than the Born-improved HEFT result, $\sigma^{NLO}_{HEFT} = 32.22^{+18\%}_{-15\%}\,\text{fb}$, and about 40% larger than the leading order result, $\sigma^{LO} = 16.72^{+28\%}_{-21\%}$. Let us note that using a leading order PDF set rather than an NLO one for the LO calculation increases the LO result by about 10%.

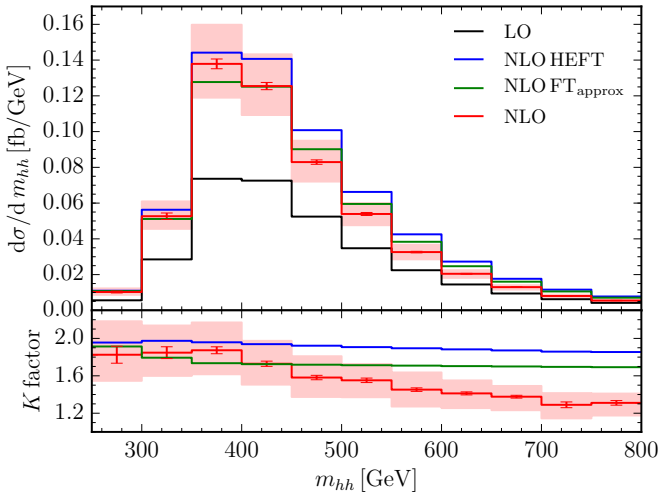

FIG. 1. Comparison of the full calculation to various approximations for the Higgs pair invariant mass distribution at $\sqrt{s} = 13\,\text{TeV}$. "NLO HEFT" denotes the effective field theory result, i.e approximation (i) above, while "FT$_{approx}$" stands for approximation (ii), where the top-quark mass is taken into account in the real radiation part only. The band results from scale variations by a factor of two around the central scale $\mu = m_{hh}/2$.

The results for the m_{hh} distribution are shown in Fig. 1. We can see that for m_{hh} beyond $\sim 450\,\text{GeV}$, the top-quark mass effects lead to a reduction of the m_{hh} distribution by about 20-30% as compared to the Born-improved HEFT approximation. We also observe that the central value of the Born-improved HEFT result lies outside the NLO scale uncertainty band of the full result for $m_{hh} \gtrsim 450\,\text{GeV}$, while the FT$_{approx}$ result, where the real radiation contains the full mass dependence, lies outside the scale uncertainty band for m_{hh} beyond $\sim 550\,\text{GeV}$. The scale uncertainty of the Born-improved HEFT and FT$_{approx}$ does not enclose the central value of the full result in the tail of the m_{hh} distribution.

In Fig. 2, we show the results for the renormalized virtual amplitude including the $\mathbf{I}$-operator as defined in Ref. [34] and compare it to various orders in an expansion in $1/m_t^2$, see Eqs. (13),(14). In the upper panel we normalize to the virtual HEFT result, while in the lower panel we normalize to the Born-improved HEFT result, i.e. $V'_N = V_N\, B/B_N$. The upper panel shows that the agreement of the full result with the HEFT result is only

good well below the threshold at $2\,m_t$. The lower one demonstrates that the deviations between the full result and the Born-improved HEFT result are more than 30% for $m_{hh} \gtrsim 480\,\text{GeV}$.

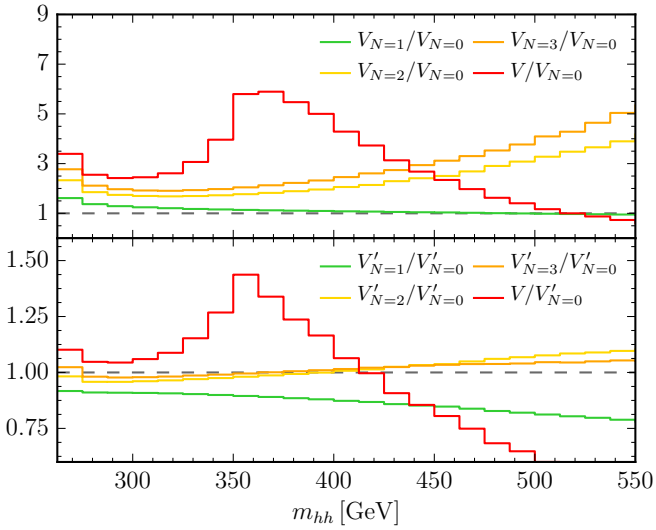

FIG. 2. Comparison of the virtual amplitude with full top-quark mass dependence to various orders in a $1/m_t^2$ expansion. V'_N denotes the Born-improved HEFT result to order N in the $1/m_t^2$ expansion, i.e. $V'_N = V_N\, B/B_N$.

CONCLUSIONS

We have calculated the total cross section and the m_{hh} distribution for Higgs boson pair production in gluon fusion at NLO, including the full top-quark mass dependence. We have also presented results for the Born-improved HEFT (Higgs Effective Field Theory) approximation, for the approximation where the virtual part is calculated in the Born-improved HEFT approximation while the real radiation part contains the full top-quark mass dependence (FT_{approx}), and for an expansion in $1/m_t^2$. We observe that the total cross section including the full top-quark mass dependence is about 14% smaller than the one obtained within the Born-improved HEFT approximation. The m_{hh} distribution shows that for m_{hh} values beyond $\sim 500\,\text{GeV}$, the top quark mass effects lead to a reduction of the differential cross section by about 20-30% as compared to the Born-improved HEFT approximation, and by about 10-20% as compared to the FT_{approx} result. Our results demonstrate that the calculation of the full top-quark mass dependence is vital in order to get reliable predictions for Higgs boson pair production over the full invariant mass range.

The method outlined here can in principle also be applied to the calculation of other multi-scale amplitudes beyond one loop.

Acknowledgements

We would like to thank Stefano Di Vita, Thomas Hahn, Stephan Jahn, Gionata Luisoni, Pierpaolo Mastrolia, Anton Stoyanov and Valery Yundin for useful discussions. We are also grateful to Andreas von Manteuffel for helpful suggestions about the use of Reduze. This research was supported in part by the Research Executive Agency (REA) of the European Union under the Grant Agreement PITN-GA2012316704 (HiggsTools) and the National Science Foundation under Grant No. NSF PHY11-25915. SB acknowledges financial support by the ERC Advanced Grant MC@NNLO (340983). NG was supported by the Swiss National Science Foundation under contract PZ00P2_154829. GH would like to acknowledge the Mainz Institute for Theoretical Physics (MITP) for its hospitality. We gratefully acknowledge support and resources provided by the Max Planck Computing and Data Facility (MPCDF).

[1] E. W. N. Glover and J. J. van der Bij, Nucl. Phys. **B309**, 282 (1988).
[2] T. Plehn, M. Spira, and P. M. Zerwas, Nucl. Phys. **B479**, 46 (1996), [Erratum: Nucl. Phys.B531,655(1998)], arXiv:hep-ph/9603205 [hep-ph].
[3] S. Dawson, S. Dittmaier, and M. Spira, Phys. Rev. **D58**, 115012 (1998), arXiv:hep-ph/9805244 [hep-ph].
[4] J. Grigo, J. Hoff, K. Melnikov, and M. Steinhauser, Nucl. Phys. **B875**, 1 (2013), arXiv:1305.7340 [hep-ph].
[5] R. Frederix, S. Frixione, V. Hirschi, F. Maltoni, O. Mattelaer, P. Torrielli, E. Vryonidou, and M. Zaro, Phys. Lett. **B732**, 142 (2014), arXiv:1401.7340 [hep-ph].
[6] J. Grigo, K. Melnikov, and M. Steinhauser, Nucl. Phys. **B888**, 17 (2014), arXiv:1408.2422 [hep-ph].
[7] F. Maltoni, E. Vryonidou, and M. Zaro, JHEP **11**, 079 (2014), arXiv:1408.6542 [hep-ph].
[8] J. Grigo, J. Hoff, and M. Steinhauser, Nucl. Phys. **B900**, 412 (2015), arXiv:1508.00909 [hep-ph].
[9] G. Degrassi, P. P. Giardino, and R. Groeber, (2016), arXiv:1603.00385 [hep-ph].
[10] D. de Florian and J. Mazzitelli, Phys. Lett. **B724**, 306 (2013), arXiv:1305.5206 [hep-ph].
[11] D. de Florian and J. Mazzitelli, Phys. Rev. Lett. **111**, 201801 (2013), arXiv:1309.6594 [hep-ph].
[12] D. Y. Shao, C. S. Li, H. T. Li, and J. Wang, JHEP **07**, 169 (2013), arXiv:1301.1245 [hep-ph].
[13] D. de Florian and J. Mazzitelli, JHEP **09**, 053 (2015), arXiv:1505.07122 [hep-ph].
[14] D. Graudenz, M. Spira, and P. M. Zerwas, Phys. Rev. Lett. **70**, 1372 (1993).
[15] M. Spira, A. Djouadi, D. Graudenz, and P. M. Zerwas, Nucl. Phys. **B453**, 17 (1995), arXiv:hep-ph/9504378 [hep-ph].
[16] R. Harlander and P. Kant, JHEP **12**, 015 (2005), arXiv:hep-ph/0509189 [hep-ph].
[17] R. V. Harlander, S. Liebler, and H. Mantler, Comput.

Phys. Commun. **184**, 1605 (2013), arXiv:1212.3249 [hep-ph].
[18] J. Carter and G. Heinrich, Comput. Phys. Commun. **182**, 1566 (2011), arXiv:1011.5493 [hep-ph].
[19] S. Borowka, J. Carter, and G. Heinrich, Comput. Phys. Commun. **184**, 396 (2013), arXiv:1204.4152 [hep-ph].
[20] S. Borowka, G. Heinrich, S. P. Jones, M. Kerner, J. Schlenk, and T. Zirke, Comput. Phys. Commun. **196**, 470 (2015), arXiv:1502.06595 [hep-ph].
[21] G. Cullen, N. Greiner, G. Heinrich, G. Luisoni, P. Mastrolia, *et al.*, Eur.Phys.J. **C72**, 1889 (2012), arXiv:1111.2034 [hep-ph].
[22] G. Cullen *et al.*, Eur. Phys. J. **C74**, 3001 (2014), arXiv:1404.7096 [hep-ph].
[23] P. Nogueira, J.Comput.Phys. **105**, 279 (1993).
[24] J. Vermaseren, (2000), arXiv:math-ph/0010025 [math-ph].
[25] J. Kuipers, T. Ueda, J. Vermaseren, and J. Vollinga, Comput.Phys.Commun. **184**, 1453 (2013), arXiv:1203.6543 [cs.SC].
[26] A. von Manteuffel and C. Studerus, (2012), arXiv:1201.4330 [hep-ph].
[27] A. V. Smirnov, Comput. Phys. Commun. **189**, 182 (2014), arXiv:1408.2372 [hep-ph].
[28] R. N. Lee, *Proceedings, 15th International Workshop on Advanced Computing and Analysis Techniques in Physics Research (ACAT 2013)*, J. Phys. Conf. Ser. **523**, 012059 (2014), arXiv:1310.1145 [hep-ph].
[29] A. von Manteuffel, E. Panzer, and R. M. Schabinger, JHEP **02**, 120 (2015), arXiv:1411.7392 [hep-ph].
[30] Z. Li, J. Wang, Q.-S. Yan, and X. Zhao, Chinese Physics C **40, No. 3**, 033103 (2016), arXiv:1508.02512 [hep-ph].
[31] J. Dick, F. Y. Kuo, and I. H. Sloan, Acta Numerica **22**, 133 (2013).
[32] D. Nuyens and R. Cools, Mathematics of Computation **75**, 903 (2006).
[33] G. P. Lepage, CLNS-80/447 (1980).
[34] S. Catani and M. H. Seymour, Nucl. Phys. **B485**, 291 (1997), [Erratum: Nucl. Phys.B510,503(1998)], arXiv:hep-ph/9605323 [hep-ph].
[35] Z. Nagy, Phys. Rev. **D68**, 094002 (2003), arXiv:hep-ph/0307268 [hep-ph].
[36] T. Hahn, Comput. Phys. Commun. **168**, 78 (2005), arXiv:hep-ph/0404043 [hep-ph].
[37] C. Anastasiou, D. de Florian, *et al.*, Report of the LHC Higgs Cross Section Working Group (2016).
[38] R. Harlander, T. Seidensticker, and M. Steinhauser, Phys. Lett. **B426**, 125 (1998), arXiv:hep-ph/9712228 [hep-ph].
[39] T. Seidensticker, (1999), arXiv:hep-ph/9905298 [hep-ph].
[40] M. Steinhauser, Comput. Phys. Commun. **134**, 335 (2001), arXiv:hep-ph/0009029 [hep-ph].
[41] J. Butterworth *et al.*, (2015), arXiv:1510.03865 [hep-ph].
[42] S. Dulat, T.-J. Hou, J. Gao, M. Guzzi, J. Huston, P. Nadolsky, J. Pumplin, C. Schmidt, D. Stump, and C. P. Yuan, Phys. Rev. **D93**, 033006 (2016), arXiv:1506.07443 [hep-ph].
[43] L. A. Harland-Lang, A. D. Martin, P. Motylinski, and R. S. Thorne, Eur. Phys. J. **C75**, 204 (2015), arXiv:1412.3989 [hep-ph].
[44] R. D. Ball *et al.* (NNPDF), JHEP **04**, 040 (2015), arXiv:1410.8849 [hep-ph].